LANGMUIR

pubs.acs.org/Langmuir Article

Novel Strategy to Enhance Human Mesenchymal Stromal Cell Immunosuppression: Harnessing Interferon-Gamma Presentation in Metal−Organic Frameworks Embedded on Heparin/Collagen Multilayers

Mahsa Haseli, Luis Pinzon-Herrera, Xiaolei Hao, S. Ranil Wickramasinghe, and Jorge Almodovar*

Cite This: https://doi.org/10.1021/acs.langmuir.3c02355 Read Online

ACCESS | Metrics & More | Article Recommendations | Supporting Information

ABSTRACT: The immunomodulatory potential of human mesenchymal stromal cells (hMSCs) can be boosted when exposed to interferon-gamma (IFN-γ). While pretreating hMSCs with IFN-γ is a common practice to enhance their immunomodulatory effects, the challenge lies in maintaining a continuous IFN-γ presence within cellular environments. Therefore, in this research, we investigate the sustainable presence of IFN-γ in the cell culture medium by immobilizing it in water-stable metal−organic frameworks (MOFs) [PCN-333(Fe)]. The immobilized IFN-γ in MOFs was coated on top of multilayers composed of combinations of heparin (HEP) and collagen (COL) that were used as a bioactive surface. Multilayers were created by using a layer-by-layer assembly technique, with the final layer alternating between collagen (COL) and heparin (HEP). We evaluated the viability, differentiation, and immunomodulatory activity of hMSCs cultured on (HEP/COL) coated with immobilized IFN-γ in MOFs after 3 and 6 days of culture. Cell viability, compared to tissue culture plastic, was not affected by immobilized IFN-γ in MOFs when they were coated on (HEP/COL) multilayers. We also verified that the osteogenic and adipogenic differentiation of the hMSCs remained unchanged. The immunomodulatory activity of hMSCs was evaluated by examining the expression of indoleamine 2,3-dioxygenase (IDO) and 11 essential immunomodulatory markers. After 6 days of culture, IDO expression and the expression of 11 immunomodulatory markers were higher in (HEP/COL) coated with immobilized IFN-γ in MOFs. Overall, (HEP/COL) multilayers coated with immobilized IFN-γ in MOFs provide a sustained presentation of cytokines to potentiate the hMSC immunomodulatory activity.

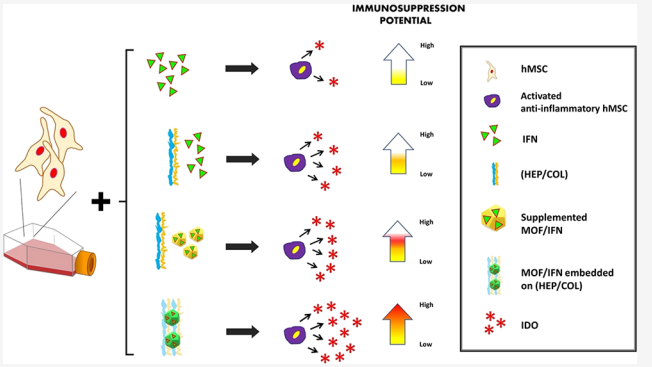

INTRODUCTION

Human mesenchymal stromal cells (hMSCs) hold significant promise for cellular therapy initiatives.[1] This type of cells possesses the ability to transform into mesodermal lineage cells, such as adipocytes, osteoblasts, and chondrocytes.[2,3] In cases of tissue damage, hMSCs demonstrate the capacity to release paracrine and anti-inflammatory substances, aiding in tissue repair.[4−6] Furthermore, these cells exhibit impressive immunomodulatory effects by generating anti-inflammatory and immunosuppressive factors.[7−12] hMSCs also prevent the activation, proliferation, and function of both adaptive immune and innate immune cells, including B cells and T cells by secreting several immunosuppressive factors.[8,13,14] The immune suppression induced by hMSCs manifests as a multifactorial process, involving both cell−cell contact and collaboration with the secretion of soluble immune factors.[15,16] Specific immune factors, such as interferon-gamma (IFN-γ), trigger the immunosuppressive response in hMSCs by stimulating the synthesis of specific protein factors, notably indoleamine-2,3-dioxygenase (IDO) and inducible nitric oxide synthase.[17−19] The expression of IDO is crucial for hMSCs to suppress T cell proliferation. Resting hMSCs do not constitutively express IDO; its expression is significantly induced when hMSCs are exposed to IFN-γ.[20] A study showed that IFN-γ can alter the immune characteristics and differentiation capabilities of hMSCs, resulting in a notable antiproliferative influence.[21] Therefore, it is important to mitigate the antiproliferative impact of IFN-γ on hMSCs.

To overcome the antiproliferative effect of IFN-γ on hMSCs, we designed polyelectrolyte multilayers via the layer-by-layer (LbL) technique. The assembly of polyelectrolyte multilayers

Received: August 14, 2023
Revised: October 20, 2023
Accepted: October 23, 2023

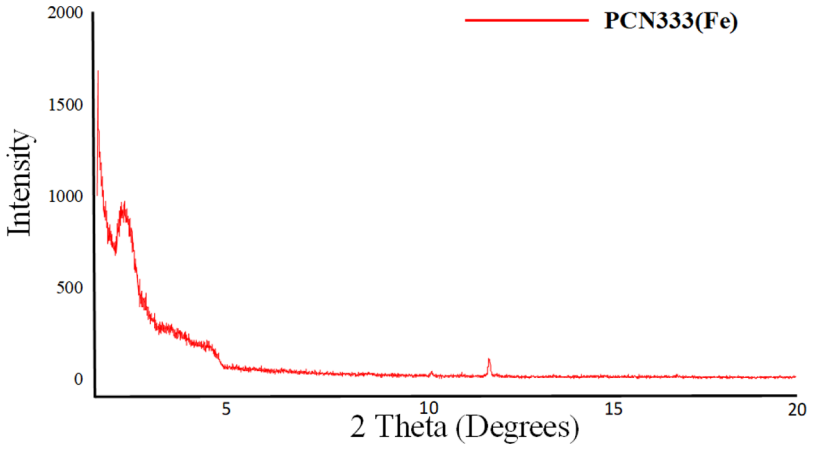

Figure 1. XRD spectra confirming synthesis of PCN-333 (Fe) (λ = 1.54178) at 25 °C.

made of heparin and collagen (HEP/COL), concluding with either COL (12 layers of HEP/COL) or HEP (13 layers of HEP/COL), has been previously demonstrated in our previous work.[22] We also confirmed that (HEP/COL) multilayers increase the immunomodulatory activity of hMSCs when the cell medium is supplemented with IFN-γ.[23] Nevertheless, pretreating hMSCs might restrict their ability to regulate immune responses effectively, as these effects could be transient and last for only a few days in specific environments.[24] We hypothesized that incorporating IFN-γ into metal−organic frameworks (MOFs) could offer a sustained release of bioactive IFN-γ. This sustained presentation may enhance the immunomodulatory activity. MOFs are crystalline materials characterized by their porous structure, involving metal-containing nodes and organic ligands.[27,47] They provide numerous advantages, including tunable yet consistent pore sizes, ultrahigh surface area, and easy modification. These features enable the immobilization of diverse molecules, such as metal complexes, nanoparticles, and proteins.[25,26] Among different types of MOFs, MOF PCN-333(Fe) exhibits a remarkable stability in aqueous solutions, a higher surface area, and ultrahigh porosity, enabling efficient loading of proteins.[27]

Here, we aim to expand on our previous work by examining the behavior of bone-marrow-derived hMSCs on polymeric multilayers coated with immobilized IFN-γ in MOFs PCN-333(Fe). We specifically examined polymeric multilayers made up of collagen (COL) and heparin (HEP), ending with either COL (12 layers of HEP/COL) or HEP (13 layers of HEP/COL). Our choice of 12 and 13 layers stems from previous findings, where we observed no differences in cell function in relation to the number of layers after 12 layers.[29] Moreover, our previous studies have established that 12 layers are the minimum required for complete surface coverage.[38] For reference, these coatings are denoted as COL and HEP, respectively.

The experiments were carried out both with and without the addition of IFN-γ in the cell culture medium serving as the control group. The arrangement involving immobilized IFN-γ in MOFs is denoted as MOFs. Furthermore, we evaluated cell behavior when hMSCs were cultured with MOFs added to the culture medium and on top of COL and HEP multilayers coated with MOFs. This evaluation was performed after 3 and 6 days of cell culture. IDO expression was measured to assess the immunomodulatory activity induced by MOFs coated on polymeric multilayers. This study specifically examined the viability and differentiation of hMSCs on polymeric multilayered surfaces containing MOFs. The results demonstrate that the coating of the MOFs did not have a negative impact on the viability and differentiation of hMSCs. Furthermore, our findings indicate that hMSCs grown on MOFs coated over HEP multilayers exhibit an enhanced capacity to sustainably present bioactive IFN-γ, thereby potentiating their immunomodulatory activity.

In summary, this study emphasizes the successful application of coating the MOFs PCN-333(Fe) onto (HEP/COL) multilayers. This technique allows for the sustained release of IFN-γ, thereby enhancing the immunomodulatory activity of hMSCs.

EXPERIMENTAL SECTION

Synthesis of PCN-333(Fe). Following the method outlined by Park et al. in 2015,[28] the precursor 4,4′,4″-s-triazine-2,4,6-triyl-tribenzoic acid (H3TATB) and MOFs PCN-333(Fe) were synthesized. A mixture of 60 mg of H3TATB, 60 mg of anhydrous $FeCl_3$ (III), 0.6 mL of TFA, and 10 mL of dimethylformamide was carried out in a 15 mL reaction vessel. A brown precipitate resulted after heating the sealed vessel in an oven at 150 °C for 12 h. The precipitate was collected through centrifugation and washed multiple times with dimethylformamide, acetone, and water. After each wash, centrifugation was performed to separate the product. Water was exchanged with acetone three times. Subsequently, the product was activated in an oven at 70 °C overnight. The product was confirmed using X-ray diffraction (XRD) on a Philips PW 1830 diffractometer with a PANalytical MPD system equipped with a Cu-sealed tube (λ = 1.54178) at 40 kV and 40 mA at 25 °C (Figure 1).

Encapsulation of IFN-γ on MOFs. A loading solution of MOFs and IFN-γ was prepared by combining them at final concentrations of 0.5 mg/mL for MOFs and 1 mg/mL for IFN-γ. The solution was diluted in Dulbecco's phosphate-buffered saline (DPBS) 1× without Ca^{2+} and Mg^{2+}, resulting in a final volume 50 μL. After vortexing, the solution was allowed to stand at 4 °C for 24 h. Subsequently, gentle centrifugation at 1000g for 1 min was performed, removing the supernatant. This step left the immobilized IFN-γ and MOFs prepared for incorporation into the cell medium.

To determine the encapsulation efficiency of immobilized IFN-γ in MOFs, the supernatant of two different batches was analyzed after 24 h of storage at 4 °C. Encapsulation was assessed using 214 nm high-performance liquid chromatography (HPLC) in a Waters HPLC system equipped with Empower 3 software and a 2695 Separations Module with an inline 2998 Photodiode Array Detector. A Cogent Bidentate C18 column was used (2.1 × 150 mm, and particle size of 4 μm). A standard curve was established using four points including 0, 0

https://doi.org/10.1021/acs.langmuir.3c02355
Langmuir XXXX, XXX, XXX−XXX

05, 0.1, and 0.2 mg/mL of IFN-γ in DPBS. The sample was injected with a volume of 20 μL.

In addition, protein quantification was assessed using the Micro BCA Protein Assay Kit (Thermo Scientific Cat#23235). According to the manufacturer, 150 μL of the sample supernatant was combined with 150 μL of working reagent prepared from the Micro BCA Protein Assay Kit in a 96-well plate. The plate was covered with foil and incubated at 37 °C for 2 h. Absorbance readings were measured at 562 nm using a BioTek Synergy 2 Multi-Mode Microplate Reader. A standard curve was set for nine points: 0, 0.25, 0.5, 1.25, 2.5, 5, 10, 20, and 100 μg/mL of IFN-γ in DPBS.[29]

The encapsulation efficiency percentage (%) was calculated using eq 1:[30]

$$\text{encapsulation efficiency\%} = \left[\frac{(C_0 - C_S)}{C_0} \times 100\right] \quad (1)$$

where C_0 is the initial concentration of INF-γ in the solution used before encapsulation and C_s is the concentration of INF-γ determined in the supernatant.

(HEP/COL) Multilayer Fabrication. (HEP/COL) multilayers were assembled using the LbL technique, as described in our previous works.[22,31−33] Heparin sodium (HEP) was bought from Smithfield BioScience (cat. no. PH300510G), and lyophilized type I collagen sponges (COL) sourced from bovine tendon (generously donated by Integra LifeSciences Holdings Corporation, Añasco, PR) were employed in constructing polymeric multilayers. These multilayers were created on sterile tissue culture-treated plates from Corning Costar (cat. no. 07-200- 740). Prior to (HEP/COL) multilayer fabrication, a strong anchoring layer was formed using poly-(ethylenimine) (PEI) (50% solution in water, $M_w \approx 750{,}000$) from Sigma-Aldrich (Cat. no. P3143).

For the coating process, PEI (1 mg/mL), HEP (1 mg/mL), and COL (1 mg/mL) were dissolved in sodium acetate buffer (at pH 5 for HEP and PEI, and at pH 4 for COL). Ultrapure water with a resistance of 18 MΩ·cm was utilized to prepare polymeric and wash solutions. This high-quality water was sourced from a Millipore-Sigma Direct-Q 3 system (cat. no. ZRQSVP3US). The washing solution was a sodium acetate buffer at pH 5. Polymeric layers were sequentially deposited and rinsed on sterile tissue culture plates through manual pipetting. The procedure began with the creation of a strong positive initial layer by depositing the PEI solution for 15 min in each well, followed by a 3 min washing with washing solution. HEP was then deposited and held for 5 min. The HEP solution was then removed, and each well was rinsed for 3 min. Next, COL was added, followed by a rinse step using the same process. This polymeric deposition and rinsing was repeated until reaching a total of 12 and 13 layers of (HEP/COL), ending in COL and HEP, respectively. The working volumes used for each solution depended on the plate size being 600 μL for 24-well plates.

After multilayer formation, MOFs were applied on top of the last layer of each coating. MOFs were dissolved in 15 mL of DPBS and coated on the surfaces for at least 1 h. After 1 h, the solution was removed and a 3 min wash was performed using DPBS. Subsequently, the substrates underwent a sterilization process using ultraviolet (UV) light for 10 min to minimize contamination before cell seeding. The working volume for MOFs also depended on the plate size being 600 μL for a 24-well plate.

Experimental Design. In this study, we investigated the cellular response of hMSCs to recombinant human IFN-γ (Thermo Fisher, catalog no. PHC4031) encapsulated inside MOFs. Ten culture conditions were examined: three groups without IFN-γ (tissue culture plastic (TCP), HEP, and COL), three groups with IFN-γ at 50 ng/mL (TCP+IFN-γ, HEP+IFN-γ, and COL+IFN-γ), and four test groups containing MOFs over HEP and COL either coated at the top of the last layer or suspended in the cell culture medium at a MOF concentration of 0.5 mg/mL. This mixture of cell medium with MOFs was made by placing MOFs (loaded with IFN-γ) in 15 mL of medium and subsequently vortexed for 1 min. The final concentration of this solution was 14.2 ng/mL of IFN-γ, as measured in our prior investigation.[34]

A 50 ng/mL concentration for soluble IFN-γ was chosen, guided by findings from our previous study.[22] Time points and the initial number of cells were selected based on the requirements and characteristics of the specific method used.

Surface Characterization. *Surface Topography via Atomic Force Microscopy.* (HEP/COL) multilayers coated with MOFs were performed on glass coverslips (size 10 × 10 mm) for future characterization. A Dimension Icon atomic force microscope (AFM) from Bruker equipped with ScanAsyst was used to characterize several properties of the coatings. *Contact in air* mode was used to analyze the topography. Using NanoScope 8.15, we measured the roughness, average roughness (Ra), and root-mean-square roughness (Rq). The analysis parameters were 512 data points per scan line for the scanning speed, 1.0 Hz for the scan frequency, and 10 × 10 μm for the size.

Surface Morphology and Chemistry via SEM/EDX. Surface morphology images were obtained using a FEI Nova NanoLab 200 scanning electron microscope (SEM) fitted with a Bruker QUANTAX EDX. Prior to imaging, each sample underwent a coating process with 10 nm of gold/palladium for 3 min.

In Situ Multilayer Formation via QCM-D. The growth of multilayers and MOF interaction with (HEP/COL) was monitored through quartz crystal microbalance with dissipation (QCM-D) measurements. These measurements were conducted using a quartz crystal microbalance with dissipation equipment from Biolin Scientific, Sweden, as described in our previous work.[32] To briefly outline the process, a mixture of deionized water, 25% ammonia solution, and 30% hydrogen peroxide solution (ratio of 5:1:1 volume part) was used to immerse the quartz at 75 °C. The cleaned quartz crystal was then placed in the QCM-D chamber. Subsequently, the PEI solution was continuously injected for 15 min at a flow rate of 100 mL/min. After the PEI injection, a sodium acetate buffer at pH 5 was introduced, as the rinse step, for 3 min supporting the same flow rate. Following this step, the HEP solution was injected for 5 min, succeeded by another injection of buffer for 3 min. The COL solution was injected for 5 min, followed again by another injection of rinse solution for 3 min. The injection of HEP and COL was alternated in the chamber (for 5 min), with an intermediate injection of sodium acetate buffer solution at pH 5 for 3 min. After 12 and 13 multilayers were built on the quartz crystal microbalance, the MOFs dissolved in DPBS at pH 7.4 were added into the chamber for 1 h. During the whole process, we recorded the frequency shift ($-\Delta F$) and dissipation (ΔD) vs time.

Cell Culture. Bone-marrow-derived hMSCs, from RoosterBio (cat. no. MSC-003), were used between passages 4 and 6. These cells were sourced from a healthy 25-year-old male donor (lot no. 00174). As per the product specification sheet, these hMSCs were positive for CD90 and CD166, which serve as identity markers for hMSCs, as confirmed through flow cytometry. They also tested negative for CD45 and CD34, indicating the absence of contamination with hematopoietic cells. Additionally, these cells demonstrated the ability to differentiate into osteogenic and adipogenic cells. The hMSCs were cultured in alpha-minimum essential medium (MEM-Alpha, 1×) from Gibco, supplemented with L-glutamine, ribonucleosides, and deoxyribonucleosides (cat. no. 12561-056) and containing 20% fetal bovine serum (FBS) from Gibco (cat. no. 12662029). The medium was further supplemented with 1.2% penicillin−streptomycin from Corning (catalog no. 30002CI) and 1.2% L-glutamine from Corning (cat. no. 25005CI).

Cell Viability. The PrestoBlue cell viability assay from Invitrogen (catalog no. A13261) was used to measure hMSC viability when cultured on the test surfaces. hMSCs were seeded at a density of 10,000 cells/cm^2 on the different conditions within a 96-well plate. Cell viability was assessed after 3 and 6 days of culture, following the methods outlined in our previous publications.[33,35,36] In brief, the cell culture medium was aspirated and 100 μL of a mixture containing 90% fresh medium and 10% PrestoBlue reagent was added to each well. The plate was then incubated for 3 h, and fluorescence intensity

https://doi.org/10.1021/acs.langmuir.3c02355
Langmuir XXXX, XXX, XXX−XXX

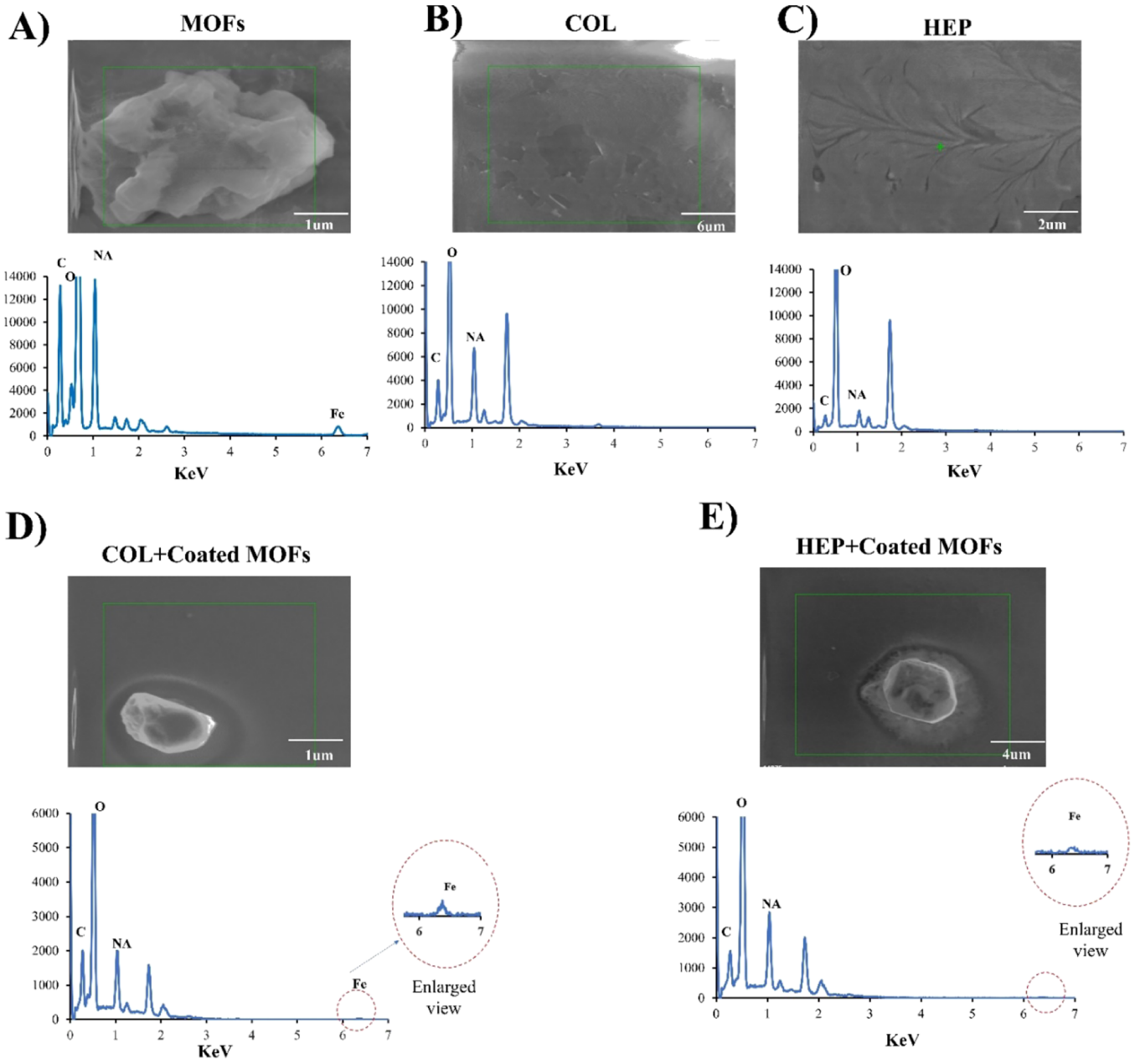

Figure 2. SEM image with EDX mapping confirms the presence of MOF on the (HEP/COL) coatings. (A) SEM/EDX of MOFs. (B, C) SEM/EDX of collagen (B) or heparin (C) terminated coatings without MOFs. (D, E) SEM/EDX of collagen (D) or heparin (E) terminated coatings with MOFs as the final layer. The presence of iron (Fe) confirms that MOFs were incorporated as the final layer of the HEP/COL coatings.

was measured using a BioTek Multi-Mode Microplate Reader (Model Synergy 2) with excitation/emission wavelengths of 560/590 nm. Data were compiled for each specific culture condition.

Fluorescent Staining. Cell nuclei and actin cytoskeleton were visualized using fluorescent dyes, specifically Hoechst 33342 (Invitrogen, ref. no. H3570) for nuclei and ActinRed 555 Ready Probest (Invitrogen, ref. no. 37112) for actin. After 3 days of cell culture, the cell medium was aspirated and the cells were fixed in a 4% formaldehyde solution for 15 min. The samples were then washed several times with DPBS (Dulbecco's phosphate-buffered saline) and treated with Triton X-100 solution for 10 min. Following this, Triton X-100 was removed and the samples were washed thrice with DPBS. ActinRed 555 dye was applied, incubated for 30 min, and protected from light using aluminum foil. After removing the ActinRed 555 and washing again for a total of five times with DPBS, 1:1000 Hoechst 33342 solution was added for 10 min and the wells were also protected from light. Next, Hoechst 33342 was removed and fixed cells were washed five times with DPBS. For cell imaging, a Leica DM IL LED Fluo inverted microscope was used with a standard DAPI filter (excitation/emission of 350/461 nm) for Hoechst 33342 and a standard TRITC filter (excitation/emission of 540/565 nm) for ActinRed 555.

Immunomodulatory Factor Expression of hMSCs. To investigate hMSC immunomodulatory factor expression, hMSCs were seeded at a density of 5000 cells/cm^2 on different test surfaces in a 24-well plate. IDO activity was assessed after 3 and 6 days of culture without changing the cell medium, following methodologies described in our prior studies.[32,33,35] In brief, 100 μL of cell supernatant was mixed with 100 μL of a standard assay mixture containing potassium phosphate buffer (50 mM, pH 6.5), ascorbic acid (40 mM, neutralized with NaOH), catalase (200 μg/mL), methylene blue (20 μM), and L-tryptophan (400 μM). This mixture was then incubated at 37 °C in a humidified incubator with 5% CO_2 for 30 min in a dark environment to protect solutions from light, allowing IDO to

https://doi.org/10.1021/acs.langmuir.3c02355
Langmuir XXXX, XXX, XXX−XXX

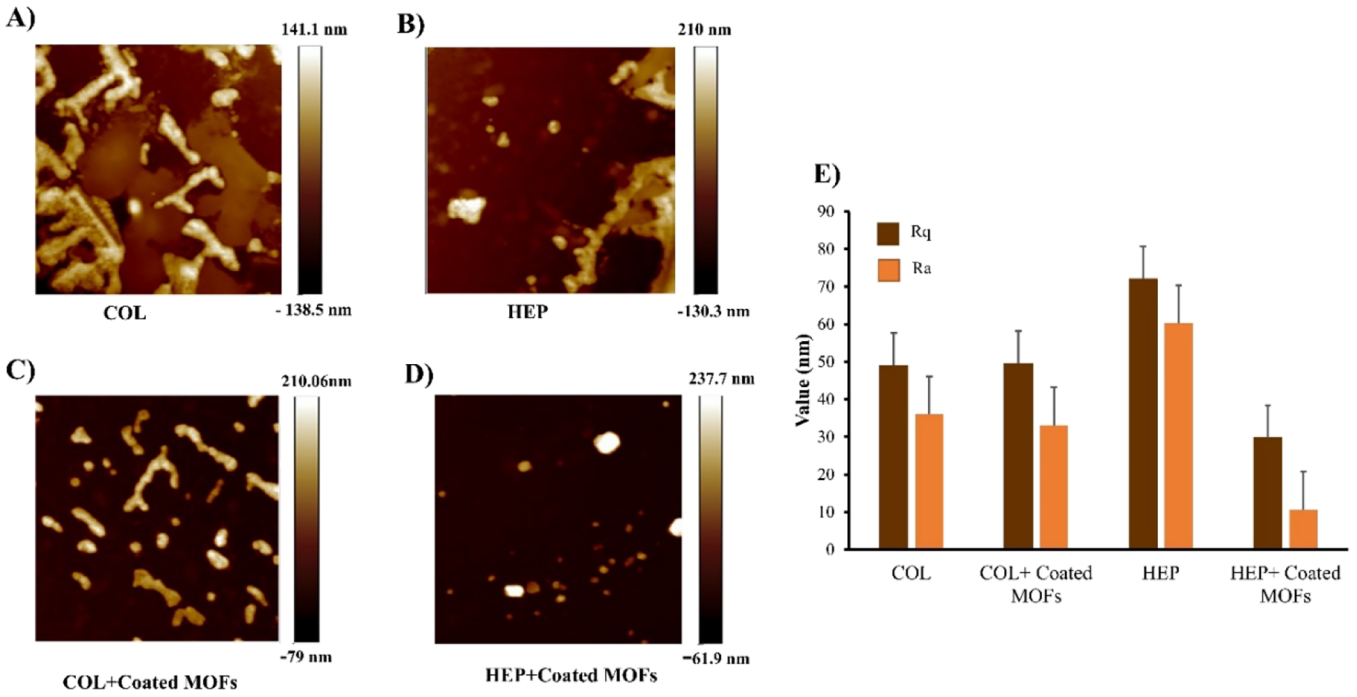

Figure 3. Surface morphology, as measured by AFM. (A) Surface morphology of a COL-terminated surface. (B) Surface morphology of a HEP-terminated surface. (C) Surface morphology of a COL-terminated surface with MOFs. (D) Surface morphology of a HEP-terminated surface with MOFs. (E) Roughness parameters Ra and Rq (nm) as a function of surface condition.

convert -tryptophan to *N*-formyl-kynurenine. The reaction was halted by adding 100 μL of 30% (wt/vol) trichloroacetic acid and incubating for 30 min at 58 °C. Following hydrolysis of *N*-formyl-kynurenine to kynurenine, 100 μL of the mixed cell supernatant/standard was transferred into a well of a 96-well microplate. Then, 100 μL of 2% (w/v) *p*-dimethylaminobenzaldehyde solution dissolved in acetic acid was added per well. Absorbance at 490 nm was measured at the end point using a BioTek Synergy 2 spectrophotometer (Synergy LX Multi-Mode Reader from BioTek Model SLXFA).

Cell Differentiation Assay. Differentiation of hMSCs was induced by incubating them in specific differentiation media, namely, osteogenic and adipogenic media. Initially, control cultures were maintained in a standard cell expansion medium. To initiate the differentiation process, hMSCs (10,000 cells/cm^2) were seeded onto surfaces prepared in 24-well plates and cultured for 6 days under the same conditions previously established in Section 2.6. Once the cell confluency reached at least 50%, the cells were exposed to the differentiation medium. For osteogenic differentiation, hMSCs were cultured in low-glucose Dulbecco's modified Eagle's medium (DMEM) with 10% FBS, 1% penicillin, 1% L-glutamine, 50 μM ascorbic acid, 10 mM β-glycerophosphate, and 100 nM dexamethasone. The medium was replaced every 2−3 days. After 8 days, the cells were fixed with 10% formaldehyde. To confirm osteogenic differentiation, cells were stained with Alizarin Red S solution and the presence of calcium deposits was observed under a microscope. Conversely, in the case of adipogenic differentiation, hMSCs were cultured in high-glucose DMEM supplemented with 10% FBS, 1% penicillin, 1% L-glutamine, 1 μM dexamethasone, 0.01 mg/mL insulin, 0.5 mM 3-isobutyl-1-methylxanthine (IBMX), and 100 μM indomethacin. The medium was also replaced every 2−3 days. After 8 days, the cells were fixed with 10% formaldehyde, stained with 0.5% (w/v) Oil Red O solution in 100% isopropanol, and inspected under a light microscope to visualize lipid vesicles, visible as bright-red spots.

Effect of Immobilized IFN-γ in MOFs on hMSC Protein Expression. An Invitrogen Th1/Th2 Cytokine 11-Plex Human Kit (assay ID: EPX110108010) was used to determine the hMSCs' protein expression. This kit was designed to assess a total of 11 analytes quantitatively. Analysis was carried out on a Luminex MAGPIX instrument. For this, hMSCs at a density of 5000 cells/cm^2 were seeded in a 96-well cell culture plate and grown for 3 days. Next, 500 μL of supernatant from the culture medium of each evaluated condition and control was collected and stored in a freezer at −80 °C until the analysis day. On the analysis day, samples were gently thawed on ice, vortexed for 30 s, and then centrifuged at 2000*g* for 1 min. Subsequently, 50 μL of each sample was analyzed following the protocol outlined by the kit.

Statistical Analysis. The results were displayed as the mean ± standard error of the mean. Statistical comparisons among multiple groups were conducted using the one-way analysis of variance (ANOVA). A *p*-value of less than 0.05 was deemed statistically significant, indicating meaningful differences between the groups.

RESULTS AND DISCUSSION

Characterization of MOFs and Polyelectrolyte Multilayers. The successful PCN-333(Fe) synthesis was confirmed via XRD at 25 °C, as depicted in Figure 1, exhibiting a pattern consistent with our previous works by Phipps et al.[37] Figure 2 presents an enlarged SEM image with EDX mapping, revealing the anticipated crystal morphology of the MOFs. The detection of iron (Fe) and the observed increase in the carbon peak (C) suggest the successful integration of MOFs on the (HEP/COL) multilayers, aligning with the findings of a study conducted by Park et al.[28]

The topography of (HEP/COL) multilayers, both coated and noncoated with MOFs, was investigated by AFM. Figure 3 presents the topographic images, revealing interesting findings. The figure showed that HEP exhibits larger clusters on the surface compared to COL, indicating significant accumulation associated with surface deposition; this observation is consistent with our previous study conducted by Haseli.[23]

On the other hand, when examining the surfaces coated with MOFs, as shown in Figure 3, it is evident that both COL and HEP coated with MOFs exhibit reduced roughness compared to their noncoated counterparts. Specifically, the roughness decreases from Ra 36 to 33.1 nm for COL and from 60 to 10.8

https://doi.org/10.1021/acs.langmuir.3c02355
Langmuir XXXX, XXX, XXX−XXX

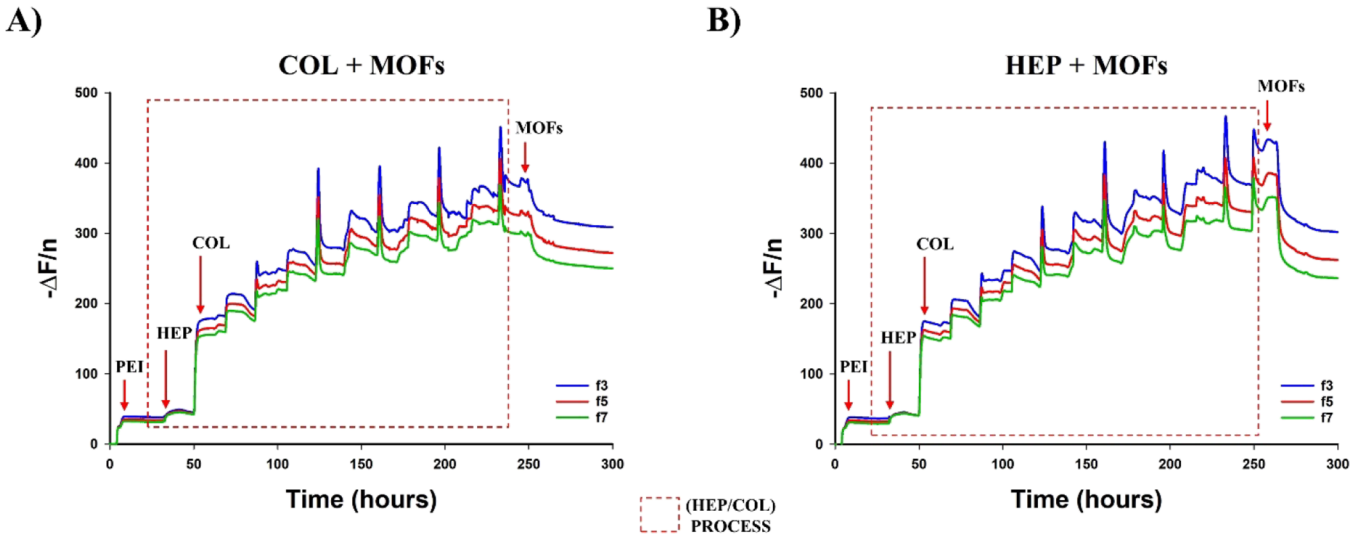

Figure 4. QCM-D data demonstrating the normalized frequency shift over time for the third, fifth, and seventh overtones during the construction of the COL-ending and HEP-ending multilayers coated with MOFs. The construction process involved alternating 3 min rinse and 5 min adsorption intervals. (A) and (B) represent the COL-ending and HEP-ending multilayers with MOF addition, respectively.

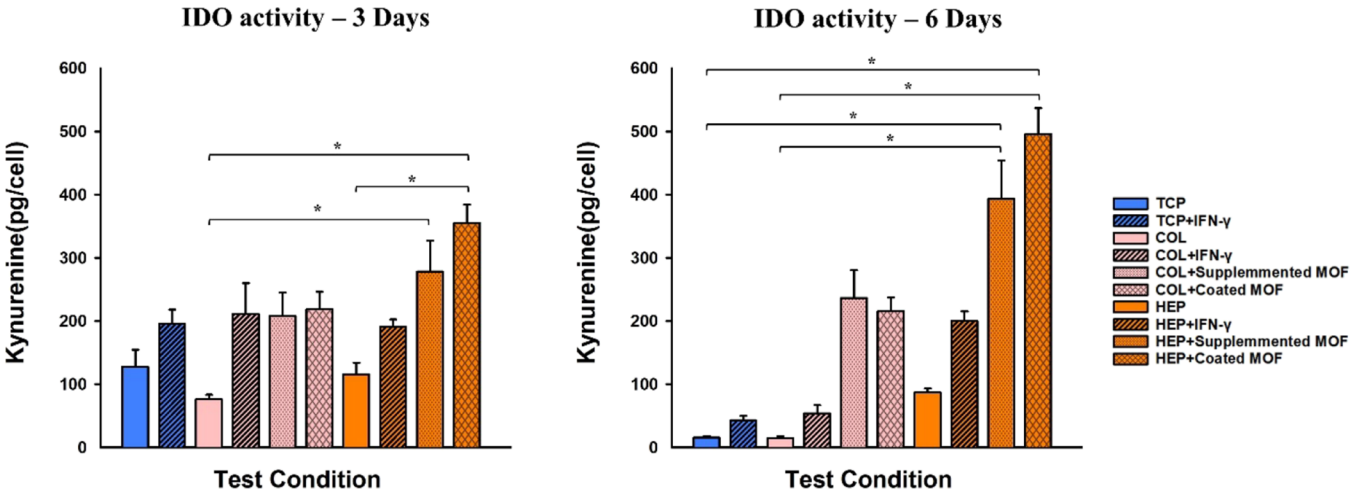

Figure 5. Immunomodulatory potential of hMSCs assessed through IDO activity. The measured kynurenine in picograms produced by cells cultured for 3 and 6 days under different experimental conditions. Data are presented as the mean ± standard deviation of $n = 4$ samples. p-values <0.05 are represented by *.

nm for HEP after MOF coating. The results show that samples with COL- or HEP-ending surfaces have a reduced roughness after the incorporation of MOFs as the final layer. It is possible that the MOFs fill the gaps between the surface features, resulting in a more uniform and smoother surface. These findings align with a study conducted by De et al.,[38] underscoring that low roughness values signify a uniform buildup and conformal coating of the substrate. Additionally, the successful attachment of MOFs to the surface leads to a uniform surface, further supporting the reduction in surface roughness.[38] These AFM results corroborate the assumptions obtained from the QCM-D results shown below, which indicated the formation of a soft layer after the deposition of MOFs. The combined evidence from both techniques suggests that the incorporation of MOFs into the (HEP/COL) multilayers results in a smoother and more uniform surface.

QCM-D was used to monitor the formation of the HEP/COL multilayers in situ and to confirm the incorporation of MOFs into the multilayers. Utilizing the detection of resonant frequency shift ($-\Delta F$) and measuring the dissipation factor (ΔD),[39] QCM-D enables the exploration of physical structures, including adsorbed mass and viscoelastic properties of multilayers.[39,40] In Figure 4, the normalized frequency shift ($-\Delta F/n$) for the third, fourth, and seventh overtones is displayed for (HEP/COL) coated with MOFs. Dissipation shift (ΔD) results are shown in Figure S1 of the Supporting Information. PEI absorption is shown in the initial 15 min, followed by a 3 min rinsing step, as depicted in Figure 4. The increase in $-\Delta F$ and ΔD during each sequential deposition of (HEP/COL) shows that the multilayers are being successfully deposited on the quartz crystal.[23,41] An increase in $-\Delta F$ was also observed, and it corresponds to an increase in the mass of deposited multilayers while an increase in ΔD indicates an enhancement in the viscoelastic structure of the deposited multilayers.[42] Thus, a rough layer on the quartz crystal exhibits a lower $-\Delta F$ whereas a dense layer exhibits a higher ΔD value. Previous reports have indicated that the Sauerbrey equation, which relates to the frequency change to mass uptake, is not

https://doi.org/10.1021/acs.langmuir.3c02355
Langmuir XXXX, XXX, XXX−XXX

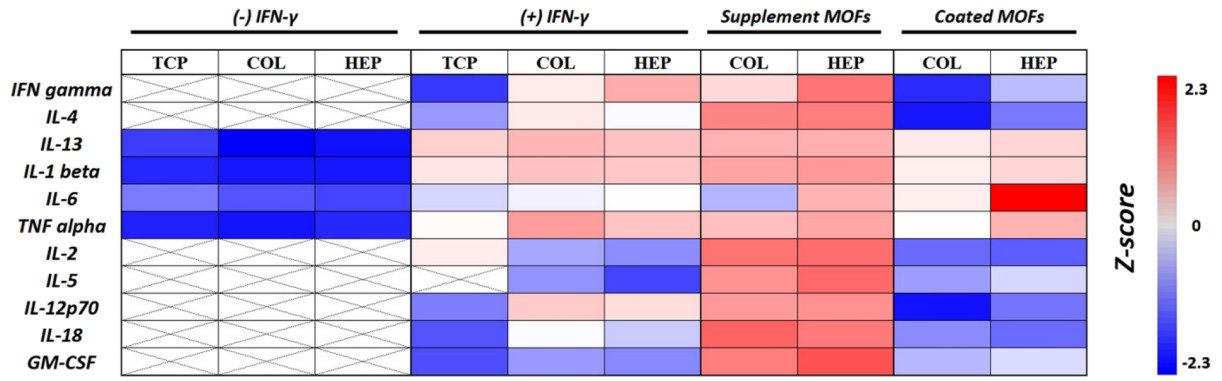

Figure 6. Protein expression of hMSCs in response to 3 days of cell culture under different conditions is depicted in the heatmap. The heatmap illustrates the *Z*-score values of 11 human cytokines. Data are presented as the mean of $n = 3$ samples.

valid for (HEP/COL) multilayers, suggesting that the film exhibits a more viscoelastic behavior with a linear mass increase over time.[23] Upon the deposition of MOFs, both $-\Delta F$ and ΔD exhibit a slight decrease in both HEP and COL-ending multilayers, indicating a negligible adsorption of the MOFs. Notably, the absorption of MOFs shows a lower $-\Delta F$ when coated on top of the COL ending compared to the HEP ending. This finding aligns with the AFM results, which demonstrate that the assembly of MOFs reduces the roughness of the layers. Subsequent to the adsorption of MOFs, a rapid decrease in the frequency shifts is observed for both COL and HEP-ending coatings, attributable to the buffer effect.[41] These results affirm the good stability of the (HEP/COL) multilayers in the presence of MOFs.

Encapsulation Efficiency of IFN-γ with PCN-333(Fe). The encapsulation efficiency of IFN-γ loaded in PCN-333(Fe) was determined using both the micro-BCA assay and HPLC. According to the results, the average percentage of IFN-γ encapsulation in PCN-333(Fe) was found to be 60 and 76% based on HPLC analysis and the micro-BCA assay, respectively. These findings indicate that PCN-333(Fe) exhibits a high loading capacity for IFN-γ, which is in line with a study conducted by Chen et al.[25]

IDO Expression. Indoleamine 2,3-dioxygenase (IDO) is a cytosolic heme protein crucial for immuno-regulatory functions.[43,44] The presence of IDO can be established by quantifying the amount of kynurenine (pg/cell) generated by cells in the presence of IFN-γ. This cytokine acts as a catalyst, converting L-tryptophan to kynurenine.[43,45] To assess the initiation of IDO expression in hMSCs, the ability of IFN-γ to stimulate IDO production was compared in all samples after 3 and 6 days. TCP without IFN-γ was selected as the control. The summarized results of the IDO activity are presented in Figure 5, demonstrating that the addition of IFN-γ to the cell medium increases the IDO activity compared to the control condition. These findings are consistent with the study by Kwee et al., which indicates a correlation between IDO activity and the amount of IFN-γ.[46] However, the IDO activity decreases after 6 days, both under TCP and TCP+IFN-γ conditions (eightfold decrease in IDO expression). Additionally, COL and HEP samples with and without IFN-γ exhibit a similar trend in IDO activity after 6 days, except HEP+IFN-γ, which shows the same level of IDO expression during 3 and 6 days.

Regarding (HEP/COL) multilayers coated with MOFs, the results demonstrate a higher IDO activity after 3 and 6 days compared to the control and TCP with IFN-γ. Notably, HEP +Coated MOFs display significantly increased IDO expression of approximately 500 pg/cell after 6 days, indicating successful loading of IFN-γ into the MOFs. Moreover, these results confirm the role of MOFs as a protective reservoir for IFN-γ, extending its activity for at least 6 days compared to that of soluble IFN-γ. Furthermore, the findings suggest that MOFs possess excellent coating ability in HEP as the last layer of (HEP/COL) multilayers due to their catalytic activities.[27] Therefore, HEP-ending multilayers coated with MOFs present a more favorable option for the presentation of IFN-γ.

hMSC Protein Expression. Quantification of 11 cytokines was performed to determine the effect of MOFs containing IFN-γ on hMSC protein expression. This assay involved testing all experimental conditions, including the presence and absence of IFN-γ. Figure 6 presents a heatmap displaying the *Z*-score for each analyte, while the raw results in pg/mL can be found in Figure S4 of the Supporting Information. A *Z*-score is a statistical measure that assesses the relationship between a specific value and the mean of a group of values. It generates a dimensionless number, providing valuable insights into how far and in which the individual value deviates from the mean.

After 3 days of cell culture, significant increases in the concentration of all analytes were observed under conditions that included IFN-γ. Once again, these results are consistent with our recent work, which demonstrated that the presence of IFN-γ positively influences protein expression by hMSCs.[34]

For the control group (absence of IFN-γ), only IL-1 beta, IL-6, IL-13, and TNF-alpha were detected. For this condition, the expression of the other cytokines was either negligible or nonexistent, falling below the lower detection limits of the instrument. These results are indicated with an "X" on the heatmap. Consequently, compared with the control, all other test groups containing IFN-γ exhibited an increase in the *Z*-score.

In our previous work, we established a direct relationship between the concentration of the supplemented MOFs and the enhanced expression of proteins. In this investigation, we also discovered that the contribution of IFN-γ had a significant effect on the expression of other cytokines. During the analysis, the condition with supplemented MOFs exhibited the highest concentration of IFN-γ, resulting in the highest *Z* values for the other analytes. This trend is visible in the larger concentration of the red area on the heatmap (Figure 6).

Specifically, compared to the test groups in the presence of IFN-γ, the use of supplemented MOFs led to an approximately

https://doi.org/10.1021/acs.langmuir.3c02355
Langmuir XXXX, XXX, XXX−XXX

Table 1. List of Quantitatively Assessed Analytes in the Protein Expression Study, along with Their Respective Functions

no.	protein name	abbreviation	function
1	*interferon-gamma*	*IFN-γ*	pro-inflammatory cytokine, which is mainly engaged in regulating the host defense and managing immune reactions.[47]
2	interleukin 4	IL-4	an anti-inflammatory cytokine that encourages T cell differentiation into Th2 cells and avoids the generation of inflammatory cytokines[48]
3	*interleukin 13*	IL-13	acting in a similar capacity to IL-4, this anti-inflammatory cytokine hinders inflammation and fosters tissue restoration.[49]
4	interleukin 1 beta	IL-1 beta	a pro-inflammatory cytokine responsible for orchestrating inflammation and immune responses, particularly pivotal in the initial stages of the inflammatory reaction.[50]
5	interleukin 6	IL-6	an all-encompassing cytokine with combined inflammatory and anti-inflammatory characteristics, actively participating in a variety of immune responses and acute-phase reactions.[51]
6	*tumor necrosis factor-alpha*	TNF-alpha	a pro-inflammatory cytokine that holds a central position in inflammation, apoptosis, and the regulation of the immune system.[52]
7	interleukin 2	IL-2	having multiple effects, this cytokine can either induce inflammation or suppress the immune system, depending on the circumstance. It takes charge of regulating T cell growth and immune responses.[53]
8	interleukin 5	IL-5	primarily acknowledged for driving eosinophil development and survival in allergic reactions, IL-5 also contributes to immune response control.[54]
9	*interleukin 12p70*	IL-12p70	IL-12p70, composed of IL-12A (p35) and IL-12B (p40) subunits, critically fosters Th1 immune responses, although it can also exert regulatory influences.[55]
10	*interleukin 18*	IL-18	a pro-inflammatory cytokine IL-18 that plays a dual role by activating both innate and adaptive immune responses, while also influencing the balance between Th1 and Th2 immune reactions.[56]
11	*granulocyte-macrophage colony-stimulating factor*	GM-CSF	GM-CSF displays attributes of both pro-inflammatory and immunosuppressive behavior. It takes part in propelling the differentiation and activation of myeloid cells such as neutrophils, macrophages, and dendritic cells.[57]

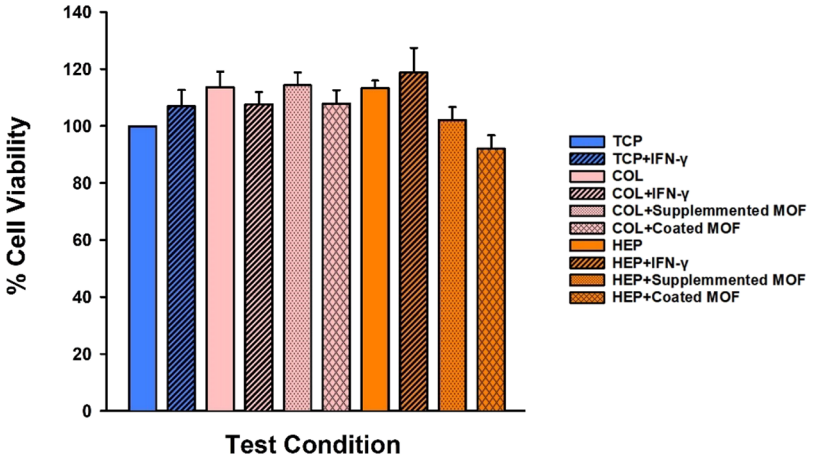

Figure 7. PrestoBlue viability assay for hMSCs after 3 days of cell culture under different experimental conditions. Data are presented as the mean ± standard deviation of $n = 5$ samples.

1.5-fold increase in IL-2 and GM-CSF expression; a nearly twofold increase in IL-5; a 10% increase in IL-1 beta, IL-4, IL-13, and IL-18; and consistent secretion levels of IL-6, IL-12p70, and TNF-alpha proteins. Alternatively, coated MOFs developed in a 10−15% reduction in IL-1 beta, IL-2, IL-4, IL-12p70, and IL-13 expression; constant expression of IL-5, GM-CSF, and TNF-alpha; and stable results for IL-6 when coated on COL. However, a 1.6-fold increase in IL-6 expression was observed when coated on HEP coatings. This decrease in expression aligns with the concentration of IFN-γ found in the coated MOF samples, which exhibited 30 and 20% decreases in IFN-γ concentration compared to the positive control for COL and HEP coatings, respectively.

In relation to the determination of IFN-γ in the samples, TCP+IFN-γ was used as the control condition. Regarding this analyte, compared to the control, both COL and HEP + IFN-γ showed increases of 38 and 50%, respectively, while the COL and HEP + supplement MOFs exhibited increases of 41 and 62%, respectively. Based on these results, it can be observed that heparin and collagen coatings promote the contribution of IFN-γ to the system, with HEP used as the final bilayer exhibiting the most significant effect among the conditions. This outcome may be attributed to the presence of loosely bound IFN-γ. For coated MOFs, only HEP showed an increase close to 22%; however, when coatings with the final bilayer as either COL or HEP were compared, the results showed an average increase of 19% in IFN-γ concentration. This increase could potentially be reflected in the expression of other analytes, where protein expression generally tended to be higher under all HEP conditions. Finally, for the condition using TCP+IFN-γ, where an initial concentration of IFN-γ of 50,000 pg/mL was introduced into the cell medium, the resulting concentration was measured at 20,800 pg/mL. This finding indicates a decrease in IFN-γ over time and in the presence of hMSC.[34]

Increase of Proteins Related to Inflammation or Dual Effect. Table 1 provides a comprehensive list of analytes quantitatively determined in the protein expression study accompanied by their corresponding functions. The table highlights whether each protein is immunosuppressive or

https://doi.org/10.1021/acs.langmuir.3c02355
Langmuir XXXX, XXX, XXX−XXX

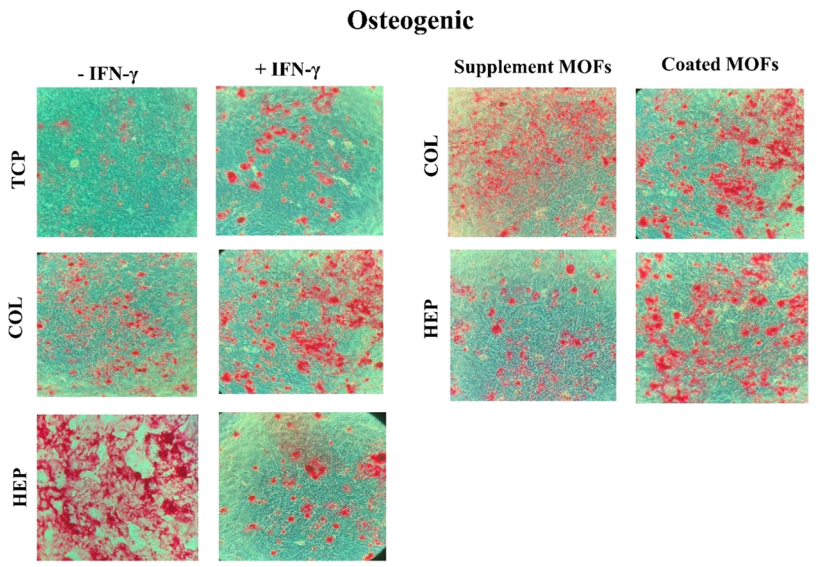

Figure 8. hMSC differentiation. Osteogenic differentiation was verified using the Alizarin Red dye, which stain calcium deposits in a vibrant red color.

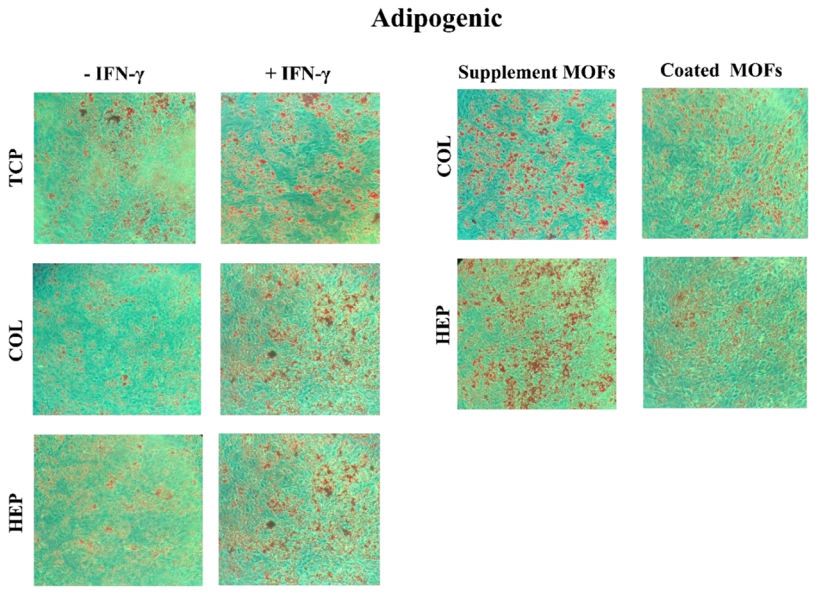

Figure 9. hMSC differentiation. Adipogenic differentiation was verified using the Oil Red dye, which stains lipid deposits red/purple.

inflammatory or exhibits dual functionality. In this study, we observed a rise in the expression of most proteins, which can be attributed to the challenges associated with controlling inflammation-related proteins while simultaneously improving the immunosuppression of hMSCs. It is important to consider that this increase may be influenced by other external factors, such as the complexity of cellular signaling, microenvironmental factors, cell-to-cell variability (due to hMSC population heterogeneity), and the dual functionality of certain proteins.

PrestoBlue Viability Assay. PrestoBlue was used for measuring cell viability after 3 and 6 days of culturing hMSCs under the different experimental and control conditions. TCP without IFN-γ was chosen as the control, and its fluorescence intensity was set as the baseline at 100%. In this way, the results of the other conditions were compared with the control assumed as normal viability at a standard in vitro culture condition.

Cell viability results demonstrated approximately 15% higher viability on COL and HEP surfaces after 3 days related to the control. Oppositely, in the case of HEP with coated MOFs, cell viability slightly decreased (Figure 7). However, ANOVA results showed that there is no evidence of significant differences in cell viability between all of the conditions after 3 and 6 days compared to the control group. These cell viability results suggest that (HEP/COL) multilayers may enhance cell viability while the presence of MOFs does not adversely affect the viability compared to the control since MOFs do not exhibit any cytotoxicity effect on hMSC. Cell viability behavior is similar for 6 days and is shown in Figure S2 in the Supporting Information.

Furthermore, fluorescence microscopy images confirmed that hMSC growth and morphology remained unaffected by the presence of (HEP/COL) multilayers or the inclusion of MOFs in solution or as the final layer, and a confluent monolayer was observed on all conditions after 72 h of culture,

https://doi.org/10.1021/acs.langmuir.3c02355
Langmuir XXXX, XXX, XXX−XXX

as indicated by actin and nuclei staining (Figure S3 in the Supporting Information).

Cell Differentiation Assay. To confirm the multipotentiality of the cells, the growth medium was replaced with a specific differentiation medium to induce hMSCs into osteogenic and adipogenic lineage cells. These differentiation assays were pivotal in assessing the capability of hMSCs to undergo lineage-specific differentiation under the indicated culture conditions. The ability to differentiate was assessed by evaluating cell functions associated with osteoblast and adipocyte differentiation after incubation for 10 days of incubation. Calcified regions and adipocyte-like cells were analyzed, and mineralization was further characterized through the microscope images.

In Figure 8 and Figure 9, areas highlighted in red and purple indicate the formation of calcified regions and adipocyte-like cells, respectively. Figure 8 demonstrates the formation of calcium deposits resulting from cell clustering, as indicated by intense Alizarin red staining for all samples, thus confirming osteogenic differentiation of cells. Likewise, Figure 9 illustrates the differentiation into adipogenic cells, transitioning from long-spindle-shaped to flattened round or polygonal cells. Notably, both Figure 8 and Figure 9 indicate that the presence of MOFs, whether added to the cell medium or applied on (HEP/COL), did not hinder the osteogenic and adipogenic differentiation of hMSCs.

CONCLUSIONS

In this research, we devised and assessed a method for the targeted delivery of IFN-γ within hMSC constructs to amplify their enduring immunomodulatory effect. To accomplish this, we employed a MOF approach, previously utilized for encapsulating enzymes.[37] The choice of MOFs as a presentation system for IFN-γ was based on their high affinity for IFN-γ and their ability to maintain protein bioactivity. These MOFs have exhibited outstanding recyclability, stability, and increased loading capacity for encapsulated enzymes.[25,37] Consistent with previous studies, MOFs exhibited good stability and efficient loading capacity for IFN-γ, aligning with the findings of Chen et al.,[25] who concluded that MOFs can successfully encapsulate cytokines. The presence of IFN-γ loaded in MOFs induced hMSC IDO expression even after 6 days of incubation under physiological conditions, surpassing the longevity of soluble IFN-γ. These results differ from a previous study that investigated the immobilization of IFN-γ to a biomimetic hydrogel, which did not extend the anticipated signaling beyond 7 days compared to soluble IFN-γ.[58] Thus, these findings suggest that MOFs are promising candidates for cytokine encapsulation.

The results of this study demonstrate the successful deposition of MOFs on (HEP/COL) multilayers. QCM-D results confirm the absorption of MOFs in each layer, while the (HEP/COL) multilayers exhibit good stability in the presence of MOFs. Importantly, this approach does not adversely affect the viability and differentiation of hMSCs in the presence of MOFs. Furthermore, the (HEP/COL) multilayers coated with MOFs provide a sustained presentation of cytokines, specifically showing an increase in the concentration of IFN-γ when HEP is used as the final bilayer. This research suggests that HEP multilayers are promising candidates for MOF coating to enhance IFN-γ presentation in the cell microenvironment. Overall, this approach has the potential to overcome the limitations of pretreatment of hMSCs by enabling a continuous presentation of IFN-γ within the cell microenvironment, thereby inducing sustained hMSC immunosuppression.

ASSOCIATED CONTENT

Supporting Information

The Supporting Information is available free of charge at https://pubs.acs.org/doi/10.1021/acs.langmuir.3c02355.

QCM-D data showing the dissipation shift as a function of time during the construction of the multilayers, viability assay for hMSCs after 6 days of cell culture, fluorescent staining of hMSC when cultured on (HEP/COL), and raw data results monitoring the effect of Immobilized IFN-γ in MOFs on hMSCs protein expression. (PDF)

AUTHOR INFORMATION

Corresponding Author

Jorge Almodovar − *Ralph E. Martin Department of Chemical Engineering, 3202 Bell Engineering Center, University of Arkansas, Fayetteville, Arkansas 72701, United States;* orcid.org/0000-0002-1151-3878; Phone: +1 479-575-3924; Email: jlalmodo@uark.edu; Fax: +1 479-575-7926

Authors

Mahsa Haseli − *Ralph E. Martin Department of Chemical Engineering, 3202 Bell Engineering Center, University of Arkansas, Fayetteville, Arkansas 72701, United States;* orcid.org/0000-0002-6593-6139

Luis Pinzon-Herrera − *Ralph E. Martin Department of Chemical Engineering, 3202 Bell Engineering Center, University of Arkansas, Fayetteville, Arkansas 72701, United States*

Xiaolei Hao − *Department of Biomedical Engineering, University of Arkansas, Fayetteville, Arkansas 72701, United States*

S. Ranil Wickramasinghe − *Ralph E. Martin Department of Chemical Engineering, 3202 Bell Engineering Center, University of Arkansas, Fayetteville, Arkansas 72701, United States*

Complete contact information is available at: https://pubs.acs.org/10.1021/acs.langmuir.3c02355

Funding

This work was financially supported in part by the National Science Foundation under grant no. 2051582.

Notes

The authors declare no competing financial interest.

ACKNOWLEDGMENTS

The authors would like to express their appreciation to the Arkansas Nano & Biomaterials Characterization Facility for granting access to the SEM and XRD instruments. Special thanks go to Dr. Walters from the University of Arkansas for providing equipment access and assistance during the quartz crystal microbalance (QCM) measurements. Additionally, the authors extend their gratitude to Integra Life Sciences for their generous donation of lyophilized Type I Collagen.

REFERENCES

(1) Ramos, T. L.; et al. MSC surface markers (CD44, CD73, and CD90) can identify human MSC-derived extracellular vesicles by

conventional flow cytometry. *Cell Commun. Signal.* **2016**, *14* (1), 1−14.
(2) Brooke, G.; et al. Therapeutic applications of mesenchymal stromal cells. *Semin. Cell Dev. Biol.* **2007**, *18* (6), 846−858.
(3) Pittenger, M. F.; Discher, D. E.; Péault, B. M.; Phinney, D. G.; Hare, J. M.; Caplan, A. I. Mesenchymal stem cell perspective: cell biology to clinical progress. *NPJ Regen. Med.* **2019**, *4* (1), 22 DOI: 10.1038/s41536-019-0083-6.
(4) Javazon, E. H.; Beggs, K. J.; Flake, A. W. Mesenchymal stem cells: Paradoxes of passaging. *Exp. Hematol.* **2004**, *32*, 414−425, DOI: 10.1016/j.exphem.2004.02.004.
(5) Rubtsov, Y. P.; Suzdaltseva, Y. G.; Goryunov, K. V.; Kalinina, N. I.; Sysoeva, V. Y.; Tkachuk, V. A. Regulation of Immunity via Multipotent Mesenchymal Stromal Cells. *Acta Naturae* **2012**, *4* (1), 23−31.
(6) Suzuki, K.; Chosa, N.; Sawada, S.; Takizawa, N.; Yaegashi, T.; Ishisaki, A. Enhancement of Anti-Inflammatory and osteogenic Abilities of Mesenchymal Stem Cells via Cell-to-Cell Adhesion to Periodontal Ligament-Derived Fibroblasts. *Stem Cells Int.* **2017**, *2017*, 3296498 DOI: 10.1155/2017/3296498.
(7) Newman, R. E.; Yoo, D.; LeRoux, M. A.; Danilkovitch-Miagkova, A. Treatment of inflammatory diseases with mesenchymal stem cells. *Inflamm. Allergy - Drug Targets* **2009**, *8* (2), 110−123.
(8) Uccelli, A.; Moretta, L.; Pistoia, V. Mesenchymal stem cells in health and disease. *Nat. Rev. Immunol.* **2008**, *8* (9), 726−736.
(9) Gao, F.; et al. Mesenchymal stem cells and immunomodulation: Current status and future prospects. *Cell Death Dis.* **2016**, *7* (1), No. e2062, DOI: 10.1038/cddis.2015.327.
(10) Frenette, P. S.; Pinho, S.; Lucas, D.; Scheiermann, C. Mesenchymal stem cell: Keystone of the hematopoietic stem cell niche and a stepping-stone for regenerative medicine. *Annu. Rev. Immunol.* **2013**, *31*, 285 DOI: 10.1146/annurev-immunol-032712-095919.
(11) Wang, Y.; Chen, X.; Cao, W.; Shi, Y. Plasticity of mesenchymal stem cells in immunomodulation: Pathological and therapeutic implications. *Nat. Immunol.* **2014**, *15* (11), 1009−1016.
(12) Ankrum, J. A.; Ong, J. F.; Karp, J. M. Mesenchymal stem cells: Immune evasive, not immune privileged. *Nat. Biotechnol.* **2014**, *32* (3), 252−260.
(13) Nauta, A. J.; Fibbe, W. E. Immunomodulatory properties of mesenchymal stromal cells. *Blood* **2007**, *110* (10), 3499−3506.
(14) English, K. Mechanisms of mesenchymal stromal cell immunomodulation. *Immunol. Cell Biol.* **2013**, *91* (1), 19−26.
(15) Cuerquis, J.; et al. Human mesenchymal stromal cells transiently increase cytokine production by activated T cells before suppressing T-cell proliferation: Effect of interferon-γ and tumor necrosis factor-α stimulation. *Cytotherapy* **2014**, *16* (2), 191−202.
(16) Kean, T. J.; Lin, P.; Caplan, A. I.; Dennis, J. E. MSCs: Delivery routes and engraftment, cell-targeting strategies, and immune modulation. *Stem Cells Int.* **2013**, *2013*, No. 732742, DOI: 10.1155/2013/732742.
(17) Gebler, A.; Zabel, O.; Seliger, B. The immunomodulatory capacity of mesenchymal stem cells. *Trends Mol. Med.* **2012**, *18* (2), 128−134.
(18) Ren, G.; et al. Mesenchymal Stem Cell-Mediated Immunosuppression Occurs via Concerted Action of Chemokines and Nitric Oxide. *Cell Stem Cell* **2008**, *2* (2), 141−150.
(19) Krampera, M.; et al. Role for Interferon-γ in the Immunomodulatory Activity of Human Bone Marrow Mesenchymal Stem Cells. *Stem Cells* **2006**, *24* (2), 386−398.
(20) Klinker, M. W.; Marklein, R. A.; Lo Surdo, J. L.; Wei, C. H.; Bauer, S. R. Morphological features of IFN-γ-stimulated mesenchymal stromal cells predict overall immunosuppressive capacity. *Proc. Natl. Acad. Sci. U. S. A.* **2017**, *114* (13), E2598−E2607.
(21) Croitoru-Lamoury, J.; Lamoury, F. M. J.; Caristo, M.; Suzuki, K.; Walker, D.; Takikawa, O.; Taylor, R.; Brew, B. J.; et al. Interferon-γ regulates the proliferation and differentiation of mesenchymal stem cells via activation of indoleamine 2,3 dioxygenase (IDO). *PLoS One* **2011**, *6* (2), No. e14698, DOI: 10.1371/journal.pone.0014698.
(22) Castilla-Casadiego, D. A.; García, J. R.; García, A. J.; Almodovar, J. Heparin/Collagen Coatings Improve Human Mesenchymal Stromal Cell Response to Interferon Gamma. *ACS Biomater. Sci. Eng.* **2019**, *5* (6), 2793−2803.
(23) Haseli, M.; et al. Immunomodulatory functions of human mesenchymal stromal cells are enhanced when cultured on HEP/COL multilayers supplemented with interferon-gamma. *Mater. Today Bio* **2022**, *13*, No. 100194.
(24) Zimmermann, J. A.; Hettiaratchi, M. H.; McDevitt, T. C. Enhanced Immunosuppression of T Cells by Sustained Presentation of Bioactive Interferon-g Within Three_Dimensional Mesenchymal Stem Cell Construct. *Stem Cells Transl. Med.* **2015**, *6*, 223−237.
(25) Chen, W.; Yang, W.; Lu, Y.; Zhu, W.; Chen, X. Encapsulation of enzyme into mesoporous cages of metal-organic frameworks for the development of highly stable electrochemical biosensors. *Anal. Methods* **2017**, *9* (21), 3213−3220.
(26) Liang, Z.; et al. A protein@metal-organic framework nanocomposite for pH-triggered anticancer drug delivery. *Dalt. Trans.* **2018**, *47* (30), 10223−10228.
(27) Feng, D.; et al. Stable metal-organic frameworks containing single-molecule traps for enzyme encapsulation. *Nat. Commun.* **2015**, *6*, 1−8.
(28) Park, J.; Feng, D.; Zhou, H. C. Dual Exchange in PCN-333: A Facile Strategy to Chemically Robust Mesoporous Chromium Metal-Organic Framework with Functional Groups. *J. Am. Chem. Soc.* **2015**, *137* (36), 11801−11809.
(29) Umrethia, M.; Kett, V. L.; Andrews, G. P.; Malcolm, R. K.; Woolfson, A. D. Selection of an analytical method for evaluating bovine serum albumin concentrations in pharmaceutical polymeric formulations. *J. Pharm. Biomed. Anal.* **2010**, *51* (5), 1175−1179.
(30) Garms, B. C.; et al. Evaluating the effect of synthesis, isolation, and characterisation variables on reported particle size and dispersity of drug loaded PLGA nanoparticles. *Mater. Adv.* **2021**, *2* (17), 5657−5671.
(31) Pinzon-Herrera, L.; Mendez-Vega, J.; Mulero-Russe, A.; Castilla-Casadiego, D. A.; Almodovar, J. Real-time monitoring of human Schwann cells on heparin-collagen coatings reveals enhanced adhesion and growth factor response. *J. Mater. Chem. B* **2020**, *8* (38), 8809−8819.
(32) Castilla-Casadiego, D. A.; et al. Methods for the Assembly and Characterization of polyelectrolyte Multilayers as Microenvironments to Modulate Human Mesenchymal Stromal Cell Response. *ACS Biomater. Sci. Eng.* **2020**, *6* (12), 6626−6651.
(33) Cifuentes, S. J.; Priyadarshani, P.; Castilla-Casadiego, D. A.; Mortensen, L. J.; Almodóvar, J.; Domenech, M. Heparin/collagen surface coatings modulate the growth, secretome, and morphology of human mesenchymal stromal cell response to interferon-gamma. *J. Biomed. Mater. Res. - Part A* **2020**, *109*, 951−965.
(34) Phipps, J.; Haseli, M.; Pinzon-Herrera, L.; Wilson, B.; Corbutt, J.; Servoss, S.; Almodovar, J.; et al. Delivery of Immobilized IFN-γ With PCN-333 and Its Effect on Human Mesenchymal Stem Cells. *ACS Biomater. Sci. Eng.* **2023**, *9*, 671 DOI: 10.1021/acsbiomaterials.2c01038.
(35) Castilla-Casadiego, D. A.; Reyes-Ramos, A. M.; Domenech, M.; Almodovar, J. Effects of Physical, Chemical, and Biological Stimulus on h-MSC Expansion and Their Functional Characteristics. *Ann. Biomed. Eng.* **2020**, *48* (2), 519−535.
(36) Pinzon-Herrera, L.; Mendez-Vega, J.; Mulero-Russe, A.; Castilla-casadiego, D. A.; Almodovar, J. Real-time monitoring of human Schwann cells on heparin-collagen coatings reveals enhanced adhesion and growth factor response. *J. Mater. Chem. B* **2020**, *8*, 8809 DOI: 10.1039/d0tb01454k.
(37) Phipps, J.; et al. Catalytic Activity, Stability, and Loading Trends of Alcohol Dehydrogenase Enzyme Encapsulated in a Metal-Organic Framework. *ACS Appl. Mater. Interfaces* **2020**, *12* (23), 26084−26094.
(38) De, S.; Nandasiri, M. I.; Schaef, H. T.; McGrail, B. P.; Nune, S. K.; Lutkenhaus, J. L. Water-Based Assembly of Polymer−Metal

https://doi.org/10.1021/acs.langmuir.3c02355
Langmuir XXXX, XXX, XXX−XXX

Organic Framework (MOF) Functional Coatings. *Adv. Mater. Interfaces* **2017**, *4* (2), 63−66.
(39) Marx, K. A. Quartz crystal microbalance: A useful tool for studying thin polymer films and complex biomolecular systems at the solution - Surface interface. *Biomacromolecules* **2003**, *4* (5), 1099−1120.
(40) Barrantes, A.; Santos, O.; Sotres, J.; Arnebrant, T. Influence of pH on the build-up of poly-L-lysine/heparin multilayers. *J. Colloid Interface Sci.* **2012**, *388* (1), 191−200.
(41) Lin, Q.; Yan, J.; Qiu, F.; Song, X.; Fu, G.; Ji, J. Heparin/collagen multilayer as a thromboresistant and endothelial favorable coating for intravascular stent. *J. Biomed. Mater. Res. - Part A* **2011**, *96 A* (1), 132−141.
(42) Easton, C. D.; Bullock, A. J.; Gigliobianco, G.; McArthur, S. L.; Macneil, S. Application of layer-by-layer coatings to tissue scaffolds-development of an angiogenic biomaterial. *J. Mater. Chem. B* **2014**, *2* (34), 5558−5568.
(43) Takikawa, O.; Kuroiwa, T.; Yamazaki, F.; Kido, R. Mechanism of interferon-γ action. Characterization of indoleamine 2,3-dioxygenase in cultured human cells induced by interferon -γ and evaluation of the enzyme-mediated tryptophan degradation in its anticellular activity. *J. Biol. Chem.* **1988**, *263* (4), 2041−2048.
(44) Mbongue, J. C.; Nicholas, D. A.; Torrez, T. W.; Kim, N. S.; Firek, A. F.; Langridge, W. H. R. The role of indoleamine 2, 3-dioxygenase in immune suppression and autoimmunity. *Vaccines* **2015**, *3* (3), 703−729.
(45) Däubener, W.; Wanagat, N.; Pilz, K.; Seghrouchni, S.; Fischer, H. G.; Hadding, U. A new, simple, bioassay for human IFN-γ. *J. Immunol. Methods* **1994**, *168* (1), 39−47.
(46) Kwee, B. J.; Lam, J.; Akue, A.; Kukuruga, M. A.; Zhang, K.; Gu, L.; Sung, K. E. Functional heterogeneity of IFN- γ − licensed mesenchymal stromal cell immunosuppressive capacity on biomaterials. *Proc. Natl. Acad. Sci.* **2021**, *118*, No. e2105972118, DOI: 10.1073/pnas.2105972118.
(47) Shtrichman, R.; Samuel, C. E. The role of gamma interferon in antimicrobial immunity. *Curr. Opin. Microbiol.* **2001**, *4* (3), 251−259.
(48) Zhang, J.; Liu, H.; Wei, B. Immune response of T cells during herpes simplex. *J. Zhejiang Univ. B* **2017**, *18* (4), 277−288.
(49) Wills-Karp, M.; Finkelman, F. D. Untangling the complex web of IL-4-and IL-13-mediated signaling pathways. *Sci. Signal.* **2008**, *1* (51), 1−5.
(50) Dinarello, C. A. A clinical perspective of IL-1β as the gatekeeper of inflammation. *Eur. J. Immunol.* **2011**, *41* (5), 1203−1217.
(51) Tanaka, T.; Kishimoto, T. Targeting interleukin-6: All the way to treat autoimmune and inflammatory diseases. *Int. J. Biol. Sci.* **2012**, *8* (9), 1227−1236.
(52) Aggarwal, B. B. Signalling pathways of the TNF superfamily: A double-edged sword. *Nat. Rev. Immunol.* **2003**, *3* (9), 745−756.
(53) Malek, T. R. The biology of interleukin-2. *Annu. Rev. Immunol.* **2008**, *26*, 453−479.
(54) Akdis, M.; Akdis, C. A. Mechanisms of allergen-specific immunotherapy: Multiple suppressor factors at work in immune tolerance to allergens. *J. Allergy Clin. Immunol.* **2014**, *133* (3), 621−631.
(55) Trinchieri, G. Interleukin-12 and the regulation of innate resistance and adaptive immunity. *Nat. Rev. Immunol.* **2003**, *3* (2), 133−146.
(56) Nakanishi, K.; Yoshimoto, T.; Tsutsui, H.; Okamura, H. Interleukin-18 Regulates Both Th1 and Th2 Responses. *Annu. Rev. Immunol.* **2001**, *19* (19), 423−474.
(57) Hamilton, J. A. GM-CSF as a target in inflammatory/autoimmune disease: Current evidence and future therapeutic potential. *Expert Rev. Clin. Immunol.* **2015**, *11* (4), 457−465.
(58) Baumann, H. J.; Betonio, P.; Abeywickrama, C. S.; Shriver, L. P.; Leipzig, N. D. Metabolomic and Signaling Programs Induced by Immobilized versus Soluble IFN γin Neural Stem Cells. *Bioconjugate Chem.* **2020**, *31* (9), 2125−2135.

https://doi.org/10.1021/acs.langmuir.3c02355
Langmuir XXXX, XXX, XXX−XXX